

Emplacement pressure conditions of Gennargentu Igneous Complex two mica granites, central Sardinia, Italy

MARIO GAETA^{1*}, LAURA MOCHI², CHIARA INVERNIZZI², AIDA MARIA CONTE³ and VALERIA MISITI⁴

¹ Dipartimento di Scienze della Terra, Università di Roma «La Sapienza», P.le A. Moro 5, I-00185 Roma, Italy

² Dipartimento di Scienze della Terra, Università di Camerino, Via Gentile III da Varano, I-62032 Camerino, Italy

³ CSES MR-CNR c/o Dipartimento di Scienze della Terra, Università di Roma «La Sapienza», P.le A. Moro 5, I-00185 Roma, Italy

⁴ Via Mogadiscio 10, I-00199 Roma, Italy

Submitted, November 1999 - Accepted, January 2000

ABSTRACT. — Scarcity of peraluminous granites in the Sardinia-Corsica batholith is a distinctive petrographic feature of this sector of the Hercynian orogenic chain. The granites of the Gennargentu Igneous Complex (hereafter GIC), completely isolated from the more common calcalkaline granites, are one of the few cases of pure crustal origin, peraluminous granite suite in Sardinia. GIC includes, in order of emplacement, three main peraluminous units: *a*) (G2M) two-mica, biotite-dominant monzogranite and granodiorite (normative corundum=2.3); *b*) (L2M) two-mica leucogranite (normative corundum=2.6); *c*) (LGM) muscovite-dominant leucogranite with andalusite and garnet (normative corundum=2.9). These granitoids were emplaced into the nappe zone at the point of maximum crustal thickening within the Sardinia segment of the Hercynian chain. Thus, study of emplacement pressure conditions of two mica granites of the GIC allowed an indirect evaluation of minimum crustal thickening.

The pressure range under which these rocks crystallised has been first inferred by microthermometric data, collected from quartz-hosted primary fluid inclusions (two main populations: 1) $T_h=300^\circ\text{C}$ and NaCl=5 wt%; 2) $T_h=330^\circ\text{C}$ and NaCl=20 wt%) from each two-mica peraluminous granites. Then, petrological

constraints based on chemical-petrographic characteristics of peraluminous GIC granites (minimum melt composition, occurrence of magmatic muscovite and andalusite), allowed to propose a more refined determination of emplacement pressure conditions. The whole data suggest that peraluminous GIC granites crystallised at a pressure of 300-400 MPa under conditions that varied from $P_{fluid} < P$ (G2M) to $P_{fluid} \approx P$ (LGM) and $a_{H_2O} \approx 1$ in the fluid.

RIASSUNTO. — La scarsità di graniti peralluminosi nel batolite Sardo-Corso è una delle caratteristiche principali che maggiormente contraddistingue questo settore della catena orogenica Ercinica. I graniti del Complesso Igneo del Gennargentu (di seguito GIC), completamente isolati dai più comuni graniti calco-alcalini, rappresentano in Sardegna una delle poche suite di graniti peralluminosi, di pura origine crostale. Il GIC è principalmente costituito, in ordine di messa in posto, da tre tipi di granitoidi peralluminosi: *a*) (G2M) monzograniti e granodioriti a due miche con biotite prevalente (corindone normativo=2,3); *b*) (L2M) leucograniti a due miche (corindone normativo=2,6); *c*) (LGM) leucograniti a muscovite dominante con andalusite e granato (corindone normativo=2,9). Questi granitoidi sono intrusi nella zona a falde, nel punto di massimo ispessimento crostale del segmento sardo della catena ercinica; conseguentemente, la determinazione della loro pressione di

* Corresponding author, E-mail: gaeta@uniroma1.it

crystallization permits an indirect evaluation of the minimum thicknesses.

The conditions of pressure in which the peraluminous GIC have crystallized have been deduced from the first place through the data of microthermometric, obtained from the analysis of the fluid inclusions (two populations principal: 1) $T_h=300^\circ\text{C}$ e $\text{NaCl}=5\%$; 2) $T_h=330^\circ\text{C}$ e $\text{NaCl}=20\%$) contained in the quartz crystals. Successively, *constraints* petrological based on the characteristic chemical-petrographic of such granitoids (composition of minimum thermal, presence of muscovite and andalusite magmatic), have permitted a more accurate determination of their pressure of intrusion. The set of data permits to define, for the peraluminous GIC, a pressure of crystallization of 300-400 MPa in conditions that vary from $P_{\text{fluid}} < P(\text{G2M})$ a $P_{\text{fluid}} \approx P(\text{LGM})$, with a $a_{\text{H}_2\text{O}} \approx 1$ in the fluid.

KEY WORDS: *Peraluminous granites, muscovite, fluid inclusions, Sardinia.*

INTRODUCTION

The pressure for granite emplacement is an important parameter for an accurate reconstruction of the tectonic history of orogenic belts into which these rocks developed (Guillot *et al.*, 1995). However, this variable is extremely difficult to estimate (Anderson, 1996).

The Hercynian Upper Carboniferous granitoids of Sardinia-Corsica batholith have been extensively studied in regard to their mineralogical, petrographic and geochemical characteristics and to delineate their possible source rocks (Tommasini *et al.*, 1995; Di Vincenzo *et al.*, 1996 and references therein). It would also be desirable to add data concerning emplacement conditions (P , T , $f\text{O}_2$, $f\text{H}_2\text{O}$) of the main granitic bodies. In fact, although the depth of intrusion, which is a function of crustal thickness, is very important in the reconstruction of the post-collisional evolution of the Hercynian chain in Sardinia, this type of data is actually non-available.

The Gennargentu Igneous Complex (hereafter GIC) is located in a nappe zone within the Hercynian chain, coinciding with the

maximum crustal thickening caused by the overthrusting of the «Internal Nappe» onto the «External Nappe». This location is ideal to estimate crustal thickness during the late phases of the Hercynian orogeny by study of pressure conditions during granite intrusion. To attain this goal, the present work was devoted to fluid inclusion studies in quartz crystals within the three different types of two-mica, peraluminous granites that form most of GIC. Abundance and size of the fluid inclusions as well as limited tectonic disturbance undergone by these granites constitute favourable factors. Furthermore, petrographic data and, especially, occurrence of andalusite and magmatic muscovite has made it possible to independently estimate the pressure and temperature range of emplacement of the peraluminous GIC granites.

This work also documents a rare peraluminous granitoid suite within the Sardinia-Corsica batholith (Cozzupoli *et al.*, 1994; Di Vincenzo *et al.*, 1996). This suite, spatially isolated from the more common calcalkaline granitoids, is similar to intrusions that form the bulk of the European Hercynian batholiths (Stussi and Cuney, 1993; Villaseca *et al.*, 1998a; Holtz and Barbey, 1991; Williamson *et al.*, 1997).

GEOLOGY OF THE STUDY AREA

The Gennargentu Mountains, central Sardinia, Italy (fig. 1), were uplifted during the Hercynian orogeny and are located south of the «Posada-Asinara Suture». This suture was generated by the Upper Devonian-Lower Carboniferous continent-continent collision that resulted in tectonic contact of the «High Grade Metamorphic Complex» with the «Low-Medium Grade Metamorphic Complex» (Carmignani *et al.*, 1992). GIC was emplaced into the nappe zone at the point of maximum crustal thickening where the «Internal Nappe» was thrust onto the «External Nappe» (thrusting of the Correboi Arc). The formations cross-cut by GIC plutonites can be subdivided

GEOLOGICAL MAP OF THE GENNARGENTU IGNEOUS COMPLEX

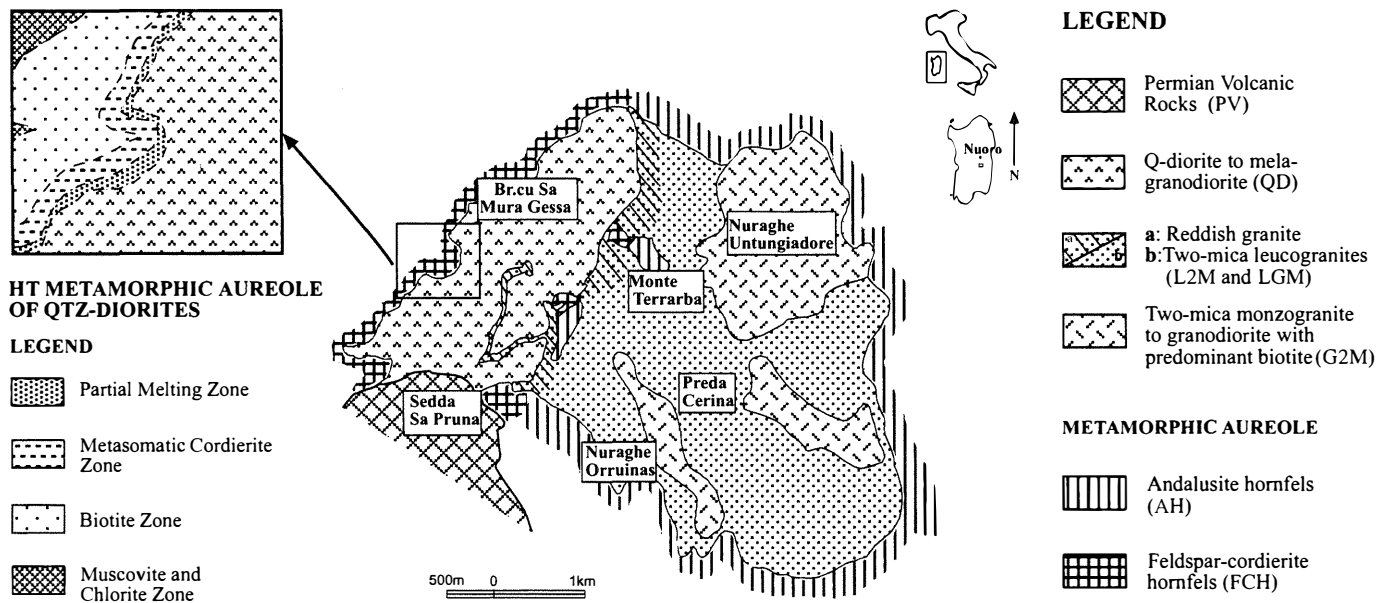


Fig. 1 – Geological map of the Gennargentu Igneous Complex.

into two distinct tectonic units: the low-grade Barbagia Metamorphic Complex and the underlying Meana Sardo Unit (Carosi and Malfatti, 1995; Carmignani, 1996). In the study area both units consist of greenschist facies metapelites.

GIC rocks comprise several lithotypes from leucogabbro to leucogranite (Cozzupoli *et al.*, 1994, 1995, 1997). The geological map of GIC (fig. 1) shows the following intrusive units, in their probable order of emplacement: *a*) two-mica, biotite-dominant monzogranite and granodiorite (G2M); *b*) two-mica leucogranite (L2M) and muscovite-dominant leucogranite with andalusite and garnet (LGM) and *c*) quartz-diorite grading into melagranodiorite (QD).

The paucity of metamorphic xenoliths within the granitoids, at the contact with the metapelitic wall rock, largely indicates passive tectonic conditions during intrusion. The metamorphic aureole (fig. 1) is apparently continuous with various types of hornfels around the entire GIC. This aureole is well marked on the western and northern margins of GIC where, in contact with QD, feldspar-cordierite hornfels (FCH), extensively injected by leucosome veins occur (Gaeta *et al.*, 1998). A reddish granite facies (sometimes with tourmaline), due to QD thermometamorphic effects, outcrop between peraluminous granitoids and QD (fig. 1). The volcanics, exposed in the south-western sector (PV in fig. 1) and directly underlying Mesozoic carbonate units, consist of pyroclastic, effusive and hypabyssal units. Field relations and geochemical characteristics of the latter two types substantiate a rooted volcanic apparatus which is cogenetic with QD (Gaeta and Palladino, in progress).

Absolute radiometric dating of GIC granitoids are not presently available. However, two ages of 255 ± 6 and 265 ± 5 Ma respectively, obtained by K-Ar method on whole-rock (Cozzupoli *et al.*, 1971a), has been determined for the Senna su Monti quartz-diorite, which is exposed less than 8 km south of the petrographically- and geochemically-

similar QD (by the way the youngest intrusion of GIC). Moreover, Cozzupoli *et al.* (1971b) report, for one sample coming from the reddish granite facies, an age of 254 ± 8 Ma (K-Ar method on separate muscovite crystals).

PETROGRAPHIC AND CHEMICAL CHARACTERISTICS OF THE TWO-MICA GRANITOIDS

GIC two mica granitoids have been distinguished in three main units based on macroscopic, textural and geochemical characteristics described below and summarised in Table 1.

Two mica granodiorite and monzogranite (G2M)

Macroscopically this group is recognised by the light colour of its feldspars, the abundance and size of unaltered biotite crystals (field-estimated colour index value of about 10 vol.%), the occurrence of rare centimetre-sized (<4 cm) «microgranular mafic enclaves» (hereafter MME) and by cross-cutting dykes of LGM.

The texture is hypidiomorphic, inequigranular and medium-grained with euhedral plagioclase and anhedral quartz which locally are more than 5 mm in length. Large crystals of quartz usually consist of subgrains, whereas some smaller crystals are optically homogeneous. When the rare crystal faces are developed at the contact between small quartz crystals and orthoclase, it is more common to observe the crystalline faces of orthoclase. Biotite crystals range from euhedral to subhedral (in contact with plagioclase) and reach a maximum size of 3 mm. Sub-millimeter-sized muscovite is generally cleanly-terminated, anhedral or rarely subhedral, with crystalline faces in contact with orthoclase and, more rarely, with quartz; sometimes it occurs as poikilitic crystals. Accessory minerals like opaque, apatite and zircon are almost always included within biotite crystals. Secondary minerals include

TABLE I
Average of the petrographic and geochemical data of GIC granitoids.

Enclaves	Texture	Grain size	Modal Abundance							Normative Abundance		Normative PI		Sr	Ba	Rb	Zr	Eu				
			Qtz	Kfs	Pl	Ms	°BA	$\frac{\text{Chl}}{\text{Chl+Bt}}$	Core	Rim	Qtz*	Kfs*	Pl*						Crn.			
G2M (13)	MME	Inequig.	< 7 mm	31	21	35	3	10	0.5	Ab ₅₆	Ab ₉₈	31	29	40	2.3	An ₂₁	1.14	180	641	198	133	6.46
L2M (8)	No	Inequig.	< 7 mm	37	25	27	6	5	0.8	Ab ₅₄	Ab ₉₈	37	30	33	2.6	An ₈	1.19	63	202	268	66	2.72
LGM (8)	No	Equig.	< 3 mm	38	24	26 ⁺	11	1	1	Ab ₉₄	Ab ₉₈	37	29	34	2.9	An ₂	1.21	24	53	322	30	2.68

() number of samples; °BA: Bt+Accessories+Chloritized Bt; ⁺Albitic plagioclase; *Normalized values; Crn: Corundum. Abbreviations of mineral names according to Kretz (1983).

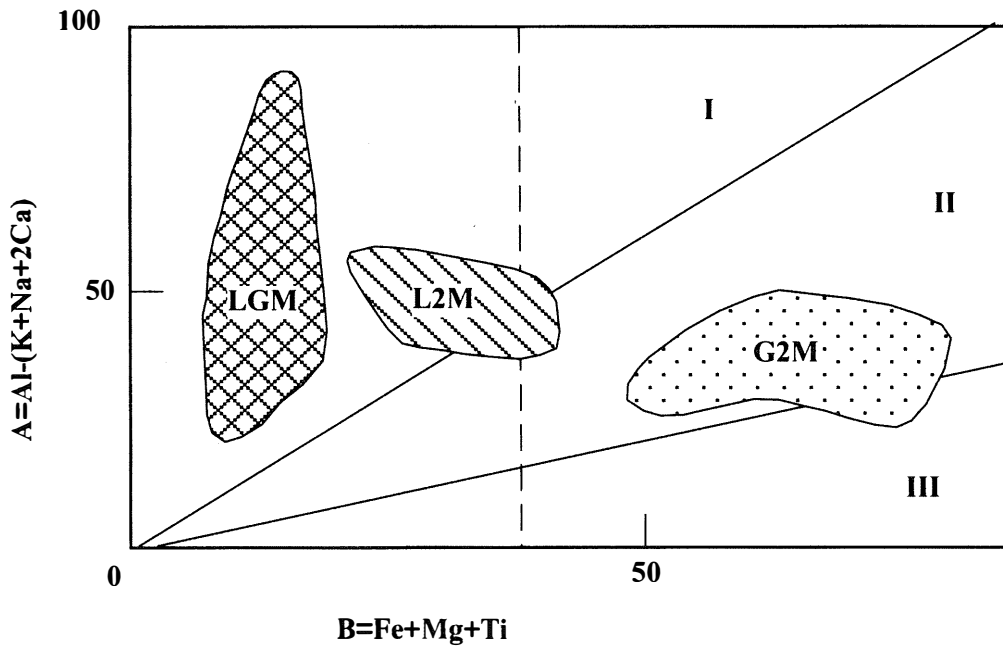


Fig. 2 – A vs B diagram (modified from Debon and Le Fort, 1983).

muscovite. Amongst the peraluminous GIC suite, this group has the highest Zr (101-156 ppm), Ba (411-921 ppm) and Sr (141-223 ppm) contents and the lowest Rb concentrations (161-265 ppm). Rb, Y and Nb contents of the G2M correspond to the syn-COLG and VAG fields on the tectonic discrimination diagram of Pearce *et al.* (1984).

Two mica leucogranite (L2M)

Macroscopically, the L2M facies is distinguished by light pink feldspar, abundant muscovite and quartz, a field-estimated colour index of around 5, and strongly chloritised biotite.

This granite is medium-grained, inequigranular, hypidiomorphic, and generally consists of subhedral (rarely euhedral) plagioclase and anhedral quartz, K-feldspar and muscovite crystals as well as subhedral, variously-chloritised biotite. Some anhedral quartz crystals greater than 5 mm consist of subgrains, whereas the smaller quartz crystals

are optically homogeneous. Muscovite is cleanly-terminated, interstitial and with the same sizes as the other phases (except for the largest quartz crystals). Chloritised biotite displays crystalline faces only in contact with plagioclase, while small, non-transformed biotite crystals are only found within the large quartz crystals. In some samples, andalusite can be found with a recognisable prismatic habit, negative elongation and, more rarely, weak pink pleochroism in the crystal core. The rare accessory minerals (opaques, apatite and zircon) are included in the biotite, while secondary white mica occurs within the core of the largest plagioclase crystals.

On the basis of modal abundances (Table 1), L2M granitoid falls in the monzogranite field of the QAP classification diagram, with a modal colour index between 2.7 and 5.9 and a quantity of muscovite between 3.8 and 7.6 vol.%.

The most common plagioclase composition is albite-oligoclase, with direct core-rim zoning in some larger crystals that again vary from

Ab₅₄ to Ab₉₈ (Table 1). Similarly to that observed in the G2M granites, microperthitic orthoclase yields Na₂O increase towards the rim.

The rare non-chloritised biotite crystals always have a high Al₂O₃/(FeO + MgO) ratio, while F, FeO and MgO contents in primary muscovite (Table 2) are lower than those found in similar rhyolite of the French Central Massif (Raimbault and Burnol, 1998) or in peraluminous granites of the eastern Arabian Shield (du Bray, 1994), both being considered as low-pressure crystalline rocks.

This granite plots in the rhyolitic field on TAS classification diagram (Le Bas *et al.*, 1986) and A/CNK ratio is between 1.08 and 1.23. In Debon and Le Fort diagram (1983), L2M plots in field I (fig. 2), which is characteristic of granitoids where muscovite prevails over biotite. Amongst the peraluminous GIC suite, this group has

intermediate Zr (45-93 ppm), Ba (122-301 ppm), Sr (47-102 ppm) and Rb (238-317 ppm) concentrations. Rb, Y and Nb contents of L2M correspond to the syn-COLG field on the tectonic discrimination diagram of Pearce *et al.* (1984).

Muscovite dominant leucogranite (LGM)

This dyke facies is leucocratic, fine-grained and rich in muscovite. LGM dykes (up to 1-3 m in width) are clearly visible in the field only when they cross-cut G2M, being difficult to distinguish from L2M.

This leucogranite is autoallotriomorphic, equigranular, isotropic and fine-grained (<1-2 mm), with some poikilitic orthoclase and muscovite crystals slightly greater than 2 mm. In addition to its size, muscovite is also distinguished for its modal abundance (Table 1). Albitic plagioclase appears to have a weak tendency towards idiomorphism, although

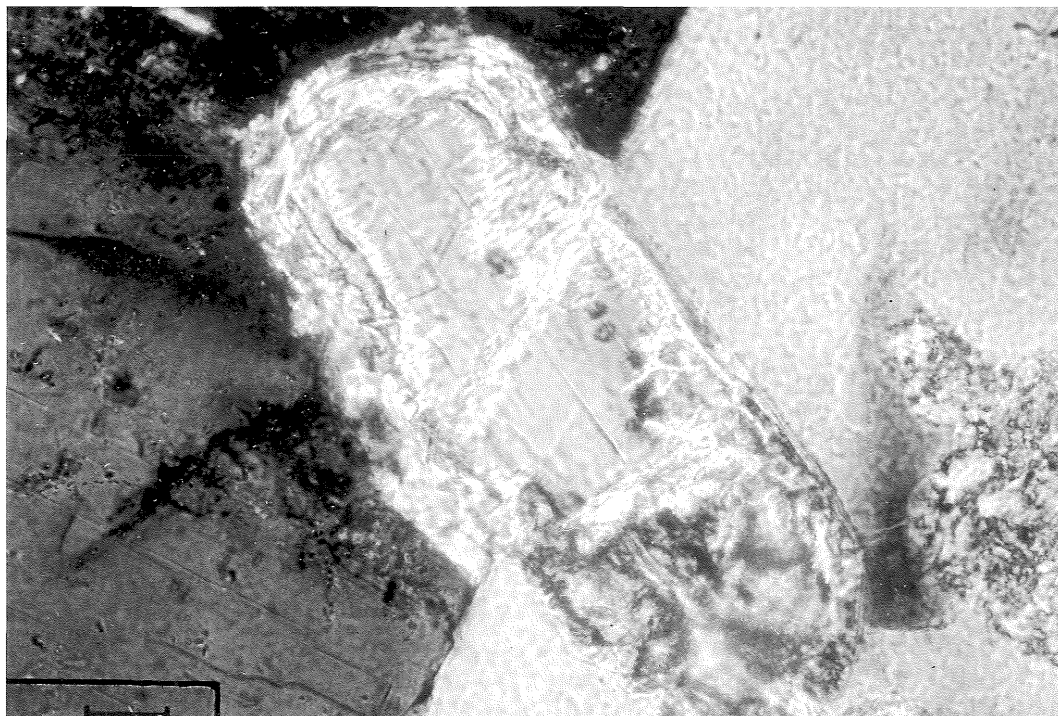


Fig. 3 – Andalusite crystal (300 μ m in size) enclosed between plagioclase (left) and muscovite (right) crystals in LGM granite ($\times 40$, crossed polarized light).

when observed in detail its contacts with quartz and orthoclase indicate crystallisation which was almost contemporaneous for the most part with the main mineral phases. Andalusite is more abundant than in L2M and occurs as sub-millimeter, subhedral crystals with rounded basal face angles; re-absorption is particularly evident when this phase is included in muscovite. In fig. 3, the difference in habit of muscovite-included and plagioclase-included andalusite crystals is obvious, with the latter indicating early andalusite crystallisation (Pichavant *et al.*, 1988). Small anhedral crystals of spessartine garnet are relatively frequent and distinctive of this granite. On the basis of modal abundances, LGM granitoid plots in the alkaline-feldspar granite field of the QAP classification diagram and has (Table 1) a modal colour index between 0.2 and 1.6 and a quantity of muscovite between 9.9 and 12.8 vol.%.

Albitic plagioclase shows a weak direct zonation, orthoclase and muscovite (Table 2) display microchemical characteristics similar to those of the other granitoids, and rare biotite is completely chloritised.

In the TAS classification diagram (Le Bas *et al.*, 1986) this rock plots in the rhyolite field, while in the Debon and Le Fort (1983) diagram it plots in the muscovite-dominant leucogranite field (fig. 2). A/CNK average is between 1.10 and 1.39. Amongst the GIC peraluminous suite, this group has the lowest contents of Zr (10-48 ppm); Ba (14-90 ppm) and Sr (9-36 ppm) and the highest Rb values (268-423 ppm). Rb, Y and Nb concentrations in L2M correspond to the syn-COLG field on the tectonic discrimination diagram of Pearce *et al.* (1984).

PRELIMINARY INDICATIONS ON THE ORIGIN AND EVOLUTION OF THE PERALUMINOUS GIC GRANITES

The occurrence of muscovite, biotite with high $Al_2O_3/(FeO + MgO)$ ratio, andalusite and garnet indicate that all GIC granites crystallised from peraluminous melts. Preliminary

geochemical data (major elements, trace elements and REE) suggest that peraluminous melts came from a source rock different from San Basilio (Sardinia, Italy) peraluminous granites (Di Vincenzo *et al.*, 1996). Although isotopic analyses were not performed in this work, a preliminary assessment of the origin of GIC melts can be given by a morphological analysis of zircon within representative samples (J.P. Pupin, pers. comm.). This analysis indicates that zircon of the peraluminous GIC suite has morphological characteristics of the crustal anatectic granite field (Pupin, 1980; Pupin, 1988).

In agreement with zircon data, most peraluminous GIC granites (in particular L2M and LGM) plot within the syn-collisional granitoid field on Rb vs Y+Nb plot (Pearce *et al.*, 1984), which is generally thought to indicate partial melting of a crustal source. It is interesting to note for comparative purposes that the calcalkaline granitoids of the Sardinia-Corsica batholith do not plot within this field, but instead plot within the VAG field (Tommasini *et al.*, 1995).

All GIC granites and granodiorites plot within the upper part (fields I and II) of the Debon and Le Fort (1983) diagram (fig. 2), which is characteristic of peraluminous rocks. GIC granitoids display a negative slope trend, as the peraluminous index $[Al-(K+Na+2Ca)]$ increases while the differentiation index $(Fe+Mg+Ti)$ decreases. This feature is analogous to that shown by *moderately peraluminous granitoids* (Villaseca *et al.*, 1998b), believed to be pure crustal magmas generated by partial melting of meta-igneous or greywacke rocks. A similar origin for peraluminous GIC granites is also indicated by the lack of basic or intermediate syn-plutonic facies.

Major elements trends, as well as representative trace elements, indicate that chemical variations in the peraluminous suite was controlled primarily by fractional crystallization of plagioclase and biotite (\pm accessories). This observation is in agreement both with the petrographic and mineral chemistry of MME, and with the major-

element mass balance results. The concept of plagioclase+biotite fractionation is also supported by strong decreases of Sr, Eu and Ba contents which are observed from G2M to LGM (Table 1). The negative correlation between Zr and SiO₂ indicates that a small amount of accessory phases (for example zircon) accompanied plagioclase and biotite during fractional crystallization process, as in the peraluminous suite of the South Mountain Batholith of Nova Scotia (Muecke and Clarke, 1981).

FLUID INCLUSION ANALYSES

A microscopic and microthermometric studies was carried out on fluid inclusions in 6 samples (two representative samples from each of the two-mica peraluminous granite types described above; i.e. G2M, L2M and LGM). It should be noted that only the quartz-hosted fluid inclusions have been examined in this study, and not the small inclusions observed in feldspars.

Approximately 100 micron-thick sections, polished on both sides, were made for each sample. Preliminary microscopic study was used to subdivide fluid inclusions into different populations on the basis of size, morphology and genesis. The microthermometric study assessed the chemico-physical characteristics of trapped fluid by measuring its eutectic, melting and homogenisation temperatures (T_e , T_{m-ice} , and T_h respectively). The phase transitions were achieved with a Reynolds gas-flux heating/cooling table (USGS) that uses liquid and gaseous nitrogen; the maximum instrument error, based on standard deviation values, was about $\pm 1.00^\circ\text{C}$. Density and salinity calculations for inclusions were performed using the Flincor program, which is based on the state equation formulated by Brown and Lamb for the H₂O-NaCl system (Brown, 1989).

Microscopic characteristics

The analysed quartz crystals were either anhedral with obvious subgrains (in particular the largest crystals) or optically homogeneous

with rare crystal faces in contact with orthoclase (usually the smallest crystals). No mosaic (dihedral angles close to 120°) or serrated-grain (typical of dynamic recrystallisation) aggregates were observed.

The abundant fluid inclusions were predominantly two-phase (liquid and vapour, L + V) and varied in size between about 5 and 50 micrometres. Three-phase-inclusions (L + V + solid) were very rarely observed.

Microscopic investigations indicated the occurrence of primary and secondary fluid inclusions in all studied samples. Primary inclusions were predominantly arranged in small groups along the boundaries of quartz grains, isolated in the interior of the crystal (fig. 4a) or, more rarely, parallel to apparent quartz crystalline faces. In addition, some large isolated inclusions were associated with groups of smaller ones which, sometimes, were arranged around it as a halo. The various types of primary fluid inclusions occupied a relatively large area of crystal surfaces, ranging in size from 20 to 50 micrometres. In general, the largest inclusions (up to 50 micrometres) were found in L2M, while the smallest (up to 20 micrometres) occur in G2M and LGM. Edges of cavities were thick, with sometimes dark colour, and their shape range from significantly irregular to elongate to «negative crystal» type. The vapour phase, which was almost always present, occupied about 30-40% of the total volume; a slight variability can be noted in the size of the vapour bubble from one inclusion to another. In LGM, however, the average percentage of vapour decrease and bubbles appeared completely absent in the smallest inclusions, while in G2M rare large single-phase primary inclusions can be found.

Secondary fluid inclusions form either intra- or inter-crystalline trails (fig. 4b). These inclusions were on average smaller (5-10 micrometer in diameter) and more transparent than primary ones, had very thin edges and were generally rounded or slightly elongate. The vapour phase was significantly reduced and occupied only around 10% of the total volume, and single-phase inclusions were rare.

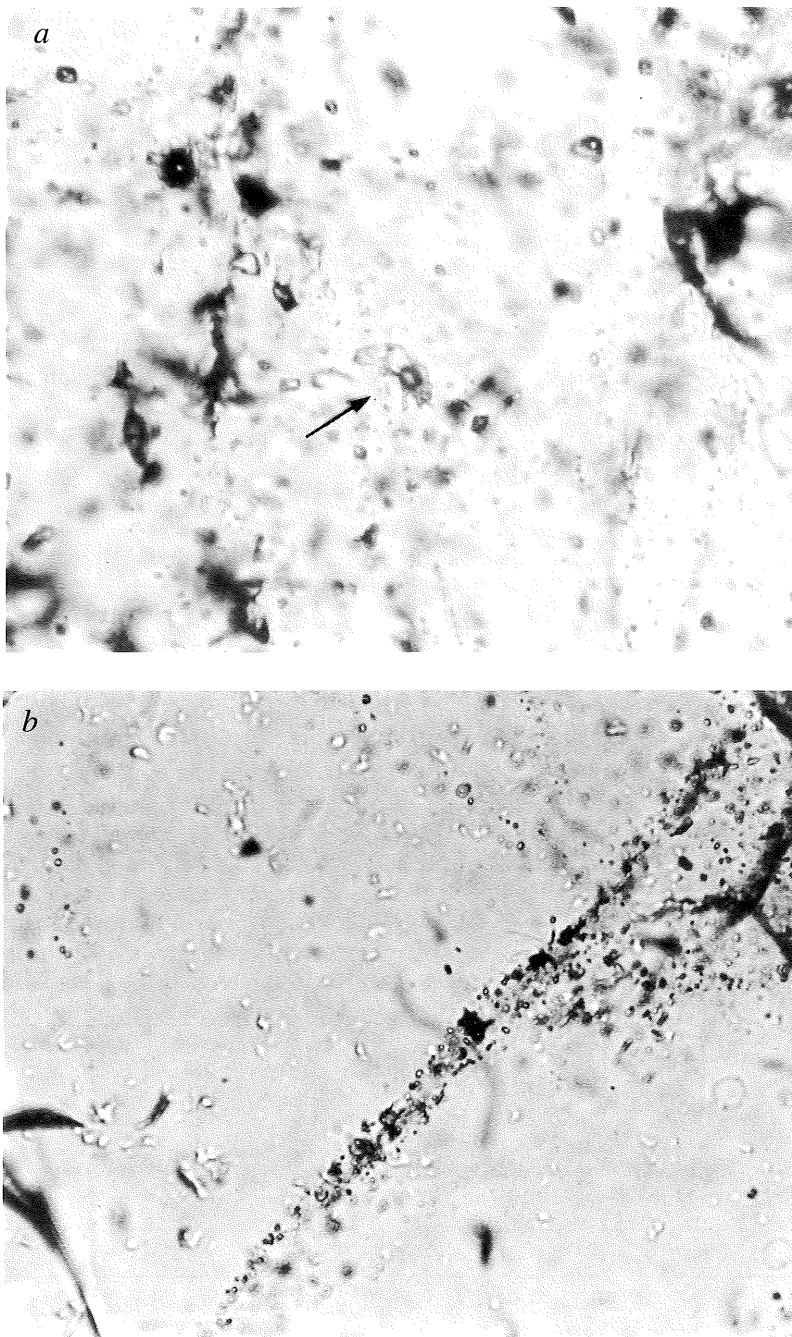


Fig. 4 – Fluid inclusions in quartz crystals of CIG granitoids. *a*) Primary inclusion in sample FL15 (L2M). The arrow indicates a 40 μm -sized inclusion ($T_h=332^\circ\text{C}$); *b*) Intracrystalline trail of secondary inclusions in sample TE280 (G2M) (magnification as in photo *a*).

Microthermometric data

A general overview of the results from the 227 primary inclusions analysed indicates that: homogenisation temperatures (T_h) range between 135° and 347°C (peak distribution between 280° and 300°C); highest eutectic temperature (T_e) is 24.4°C; melting temperatures (T_{m-ice}) are between -18.8° and 0.0°C; salinity values range from 0.0 to 21.5 wt% NaCl and density values are from 0.66 to 0.98 g/l.

G2M granodiorite (samples TE104 and TE280) shows the widest range for T_h values (Table 3), with a peak distribution observed between 260° and 280°C, while T_{m-ice} values are more restricted and salinity values are lower than in L2M and LGM. L2M (samples FL5 and FL15) and LGM (samples FL9 and TE56) granites have a very similar T_h range (Table 3), with most measurements occurring in a temperature range (280°-300°C) which is slightly higher than in G2M. T_{m-ice} range of values is also very similar for L2M and LGM granites (Table 3). Finally, it should be noted that very low T_{m-ice} values were measured only in one case in L2M and in two cases in LGM, and that these three inclusions yielded high homogenisation temperatures ($T_h=330°C$). Excluding these last inclusions, T_{m-ice} values for LGM (fig. 5) and L2M are generally clustered around -3°C, indicating together with T_e temperatures a H₂O-NaCl system with an average NaCl concentration between 4 and 6 wt%.

In general the measured parameters vary significantly in all peraluminous GIC granitoids (Table 3) and some of them, in particular T_h , can exhibit a bimodal

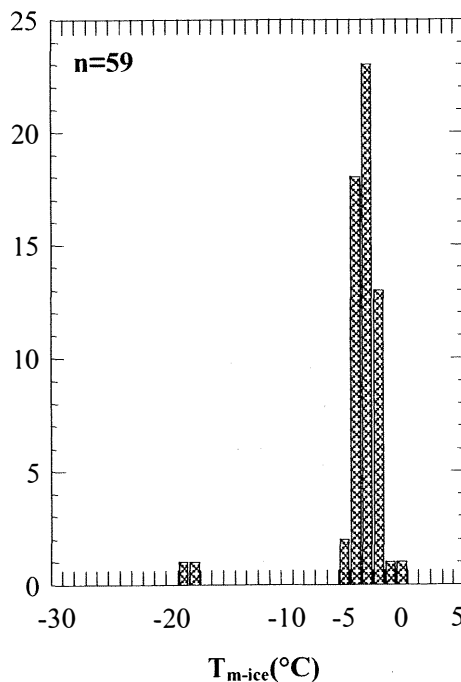


Fig. 5 – Histogram showing T_{m-ice} distribution for primary inclusions in LGM quartz crystals; n =number of measures.

distribution, as shown in fig. 6 for T_h values of LGM. As shown in this figure, a higher mode occurs at $T_h=280°-300°C$, a wider, less-pronounced mode occurs between 220° and 260°C and a minimum zone is located in between at 260°-280°C. T_h values below this minimum were generally measured in the large quartz crystals with subgrains and, in agreement with the Gallura Hercynian granites (Giorgetti *et al.*, 1992), did not appear

TABLE 3

Microthermometric data (variation range) of fluid inclusions in quartz crystals from the GIC granitoids.

	T_h (°C)	T_{m-ice} (°C)	NaCl (%)	ρ (g/l)	T_e (°C)*
G2M	135.0 ÷ 347.0	- 5.7 ÷ 0.0	8.78 ÷ 0.00	0.86 ÷ 0.78	-12.0 ÷ -22.1
L2M	197.0 ÷ 332.0	-14.7 ÷ -0.6	18.37 ÷ 0.99	0.88 ÷ 0.66	- 5.7 ÷ -22.1
LGM	204.7 ÷ 335.5	-18.8 ÷ -0.3	21.52 ÷ 0.50	0.97 ÷ 0.78	- 7.6 ÷ -24.4

* Inclusions with $T_h > 270°C$ only.

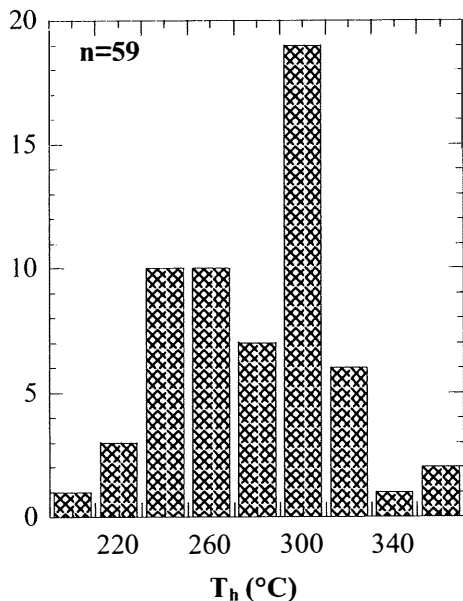


Fig. 6 – Histogram showing T_h distribution for primary inclusions in LGM quartz crystals; n =number of measures.

compatible with magmatic crystallisation of quartz. This type of low-temperature inclusion ($T_h < 270^\circ\text{C}$) is particularly concentrated in G2M, which contains, as previously mentioned, a greater concentration of large quartz crystals with subgrains and shows evidence of late fracturation (LGM dykes). Plot of L2M and LGM inclusions on a T_h vs NaCl diagram (fig. 7) displays a positive slope trend and at least two populations, with different temperatures and salinities (the third population, formed by the three highest NaCl values, have been excluded from the diagram).

Considering that evidence of subsolidus quartz re-crystallisation in the peraluminous GIC granites is non conclusive, because of the occurrence of crystals without subgrains and the random distribution of the contacts between the phases (Ashworth and McLellan, 1985), and because two fluid inclusion populations exist with T_h values significantly higher ($T_h = 300^\circ$ and $T_h = 330^\circ\text{C}$) than in calcalkaline rocks of northern Sardinia (Giorgetti *et al.*, 1992), it is likely that the quartz crystals analysed in this work host two populations of primary

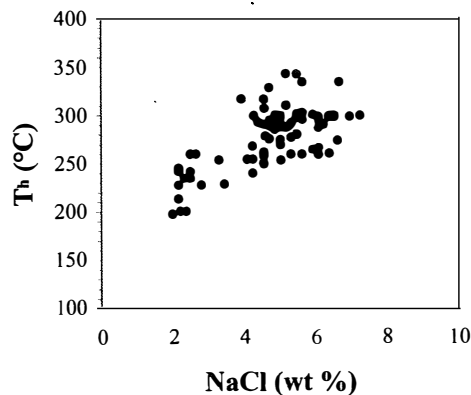


Fig. 7 – Plot of T_h vs NaCl for primary fluid inclusions in L2M and LGM quartz crystals.

inclusions containing magmatic fluids. The low salinity of the 5 wt% NaCl-population is in agreement with the bulk rock chemistry of the most differentiated GIC leucogranite (LGM), which has low Ca contents (average CaO content in LGM is 0.31 wt%).

The T_h histogram shown in fig. 8 reports the frequency of inclusions with $T_h > 270^\circ\text{C}$, indicating a maximum peak for L2M and LGM in the $290^\circ\text{--}300^\circ\text{C}$ class. On the basis of preceding considerations, the number of measurements ($n=83$) and the symmetrical distribution around the peak, the class 300°C can be considered as statistically representative of T_h of fluid inclusions formed during magmatic crystallisation of quartz (in particular those contained within the LGM). This figure also shows that the majority of G2M measures are shifted towards lower temperatures ($270 < T_h < 290^\circ\text{C}$).

The $T_h = 300^\circ\text{C}$ (H_2O -5 wt% NaCl) and $T_h = 330^\circ\text{C}$ (H_2O -20 wt% NaCl) isochores calculated by Bodnard and Vityk (1994) equation are P (MPa) = $1.05 T$ ($^\circ\text{C}$) - 315 and P (MPa) = $0.92 T$ ($^\circ\text{C}$) - 303.6 respectively (fig. 9).

DISCUSSION

From petrological constraints, along with chemical-petrographic characteristics of the peraluminous GIC granites, it is possible to infer the pressure range under which these

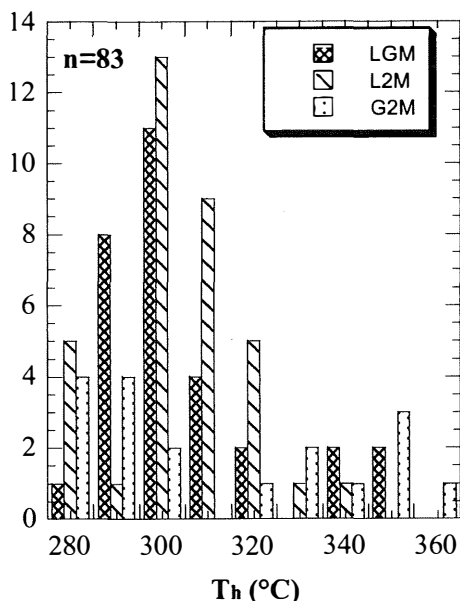


Fig. 8 – Histogram showing distribution of primary fluid inclusions having $T_h > 270^\circ\text{C}$ in quartz crystals of GIC granitoids; n =number of measures.

rocks crystallised. The microthermometric data collected from fluid inclusions were used to give a more refined determination.

High amounts of hydrous phases (maximum $\text{Bt} + \text{Ms} + \text{Chl}$ value = 16 vol.%) in G2M provide clear indication that G2M crystallised under water-bearing conditions. Inclusion relationships, grain sizes, grain shapes and mineralogical compositions of the autholithic enclaves indicate early and almost contemporaneous crystallisation of plagioclase and biotite. Considering phase relationships in two-mica leucogranite at $P = 400$ MPa (Scaillet *et al.*, 1995), a crystallisation sequence similar to that observed in G2M is only possible if water content range between 5 and 6 wt%. With $\text{H}_2\text{O} > 6$ wt%, biotite crystallises earlier than plagioclase (with a thermal gap between the onset of crystallisation of the two phases which is too large, regarding G2M petrographic evidence), while $\text{H}_2\text{O} < 5$ wt% would prevent occurrence of magmatic muscovite. Crystallisation in hydrous, but water-

undersaturated conditions is also suggested for G2M by occurrence, in many samples of abundant biotite not transformed into chlorite (Table 1).

In contrast, high chlorite/biotite ratios in L2M and LGM (Table 1) may indicate a discrete vapour phase during magmatic crystallisation. Crystallisation under subsolvus conditions at $P_{\text{H}_2\text{O}} > 220$ MPa (Smith and Brown, 1988) is certainly possible in low-CaO, peraluminous GIC granites (LGM), which always contain well developed albite and orthoclase (Table 1).

In summary, petrographic evidence reported in Table 1 and the nature of the fluids present in quartz-hosted inclusions suggest that peraluminous GIC granites crystallised under conditions ranging from $P_{\text{fluid}} < P$ (G2M) to $P_{\text{fluid}} \approx P$ (LGM) and with $a_{\text{H}_2\text{O}} \approx 1$ in the fluid.

Muscovite crystals of GIC granites, in agreement with Miller *et al.* (1981), du Bray (1994) and Raimbault and Burnol (1998), can be considered as largely primary (with minor secondary crystals) and have formed under high pressures, based on the fact that they: 1) are often cleanly terminated or, in some cases, subhedral; 2) are similar in size to other phases in L2M and LGM; 3) were formed in a strongly peraluminous system (also indicated by biotite with high $\text{Al}_2\text{O}_3/(\text{FeO} + \text{MgO})$ ratio, andalusite and garnet); 4) have high Al_2O_3 , Na_2O and TiO_2 contents and as well as low F and celadonite contents. Magmatic muscovite may indicate crystallisation at $P_{\text{H}_2\text{O}} \geq 300$ MPa if $P = P_{\text{H}_2\text{O}}$ (Althaus *et al.*, 1970; Chatterjee and Johannes, 1974; Johannes and Holtz, 1996).

Occurrence of andalusite in L2M and LGM also provides a pressure constraint for GIC granites. Lack of fibrolite and textural evidence (fig. 3) indicate that the Al_2SiO_5 polymorph crystallised directly from the melt and before muscovite. In fact, in L2M and LGM, andalusite shows a cotectic relationship with plagioclase and was involved in the reaction $\text{Al}_2\text{SiO}_5 + \text{melt} = \text{muscovite}$ during the final stages. Occurrence of magmatic andalusite indicates a maximum crystallisation pressure which was definitely less than the Al_2SiO_5

polymorph triple point around 500 MPa. The 500 MPa pressure, (Richardson *et al.*, 1969) is presently considered as the maximum value for the equilibration of the three-phase andalusite-sillimanite-kyanite assemblage (Kerrick, 1990, page 104).

Table 1 shows that the normative composition of LGM (Qtz₃₇/Alb₃₄/Kfs₂₉) is very close to the thermal minimum of the haplogranitic system (Qtz-Alb-Kfs-H₂O) if one consider the melt peraluminosity. As proposed by Holtz *et al.* (1992), the thermal minimum in the peraluminous haplogranitic system (normative corundum > 0; A/CNK>1) at P_{H₂O}=200 MPa contains a higher normative quartz content (39%) and a melting temperature lower by about 25°C than the metaluminous haplogranitic system at the same P (Tuttle and Bowen, 1958). As a first approximation, ΔQtz defined at 200 MPa was applied in the pressure range inferred by the occurrence of muscovite and andalusite (300≤P_{H₂O}≤500 MPa) to the metaluminous

haplogranitic system, because similar data are not available for the peraluminous haplogranitic system at P>200 MPa. A good correspondence exists between eutectic composition and LGM. Thus, LGM can be considered, in agreement with their textural characteristics and occurrence as dykes, as crystallisation products of a peraluminous minimum melt that was injected late into the other peraluminous GIC granitoids. If so, solidus curve of LGM granites can be considered as almost isothermal in the studied pressure range (Wyllie, 1984). Excluding expansion of the liquid field due to occurrence of F (minor in biotite and muscovite) or B (lack of tourmaline), solidus temperature can be deduced using haplogranitic system data at 300 and 500 MPa lowered by ΔT value due to peraluminosity (Holtz *et al.*, 1992).

The P-T diagram of fig. 9 shows the T_h=300°C (H₂O-5 wt% NaCl) isochore which is the most representative of primary fluid inclusions occurring in L2M and LGM, the T_h=330°C (H₂O-20 wt% NaCl) isochore which is representative of rare, highest salinity fluid inclusions occurring in L2M and LGM, the solidus curve inferred for LGM from Holtz *et al.* (1992) data, the curve for the reaction quartz+muscovite+albite=alkali feldspar+Al₂SiO₅+melt at a_{H₂O}=1 (Johannes and Holtz, 1996) and the stability fields of Al₂SiO₅ polymorphs (Richardson *et al.*, 1969). The T_h=300°C isochore and the presumed LGM solidus curve intersect within the muscovite stability field at P≈360 MPa; the T_h=330°C isochore intersect the LGM solidus curve at P≈300 MPa within the andalusite stability field and out the muscovite stability field. The convergence of data summarised in fig. 9 indicates that LGM may represent a minimum peraluminous melt which crystallised at P≈300-400 MPa in H₂O-saturated conditions (a_{H₂O}=1). The difference between the two intersection points could be due either to analytical uncertainties or to isobaric evolution of magmatic fluids. In the latter case (arrow in fig. 9), high salinity inclusions could represent fluid composition during andalusite+quartz+feldspar

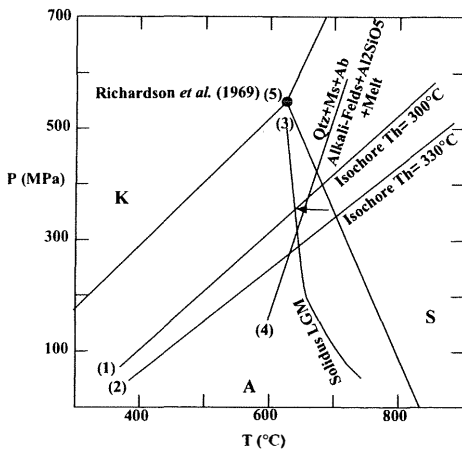


Fig. 9 – P-T diagram showing: 1) isochore T_h = 300°C (H₂O-5 wt% NaCl) (Bodnar and Vityk, 1994); 2) isochore T_h = 330°C (H₂O-20 wt% NaCl) (Bodnar and Vityk, 1994); 3) the solidus curve of LGM peraluminous melt inferred from Holtz *et al.* (1992) data; 4) the quartz+muscovite+albite=alkali feldspar+Al₂SiO₅+melt reaction curve at a_{H₂O}=1 (Johannes and Holtz, 1996); 5) the stability field of the Al₂SiO₅ polymorphs (Richardson *et al.*, 1969). A=andalusite; S=sillimanite; K=kyanite; arrow indicates the isobaric evolution of magmatic fluids (see text for more explanations).

crystallisation, while low salinity inclusions could represent fluid composition close to the solidus, when muscovite + quartz + alkali feldspar crystallised.

Syn-plutonic contacts with LGM, highly similar quartz/feldspar ratios (either modal, or normative) (Table 1), occurrence of (andalusite+muscovite) association, high Chl/(Chl+Bt) ratios and, above all, similar microthermometric values measured in fluid inclusions (Table 3 and fig. 8) indicate that L2M quartz must have crystallised from a slightly less differentiated peraluminous magma at P_{H_2O} conditions similar to LGM.

Petrographic characteristics, lack of andalusite, the reduced number of primary fluid inclusions and contrasting observed microthermometric values (fig. 8) make it unlikely that G2M crystallised under identical conditions. However, if intrusion pressure for G2M peraluminous granitic mass, was greater than that deduced for LGM and L2M ($\approx 300-400$ MPa), this would contradict the lack of garnet and staurolite within metapelites (Carmichael, 1978; Pattison and Tracy, 1991) of GIC metamorphic aureole (fig. 1). Furthermore, because G2M definitely predates LGM and has magmatic muscovite with a composition similar to L2M and LGM (Table 2), an intrusion pressure of less than 300 MPa can be excluded for this granite.

CONCLUSIONS

Scarcity of peraluminous granites in the Sardinia-Corsica batholith is one of the petrographic characteristics that make this sector of the Hercynian orogenic chain distinctive. The granites of Gennargentu Igneous Complex, completely isolated from the more common calcalkaline granites, are one of the few cases of a pure crustal origin, peraluminous suite in Sardinia. In contrast, peraluminous granites form a large part of the main European Hercynian batholiths.

On the basis of geometric relationships deduced in the field, chemical-petrographic characteristics and petrographic/microthermometric measurements performed on fluid inclusions, the following model for intrusion of the peraluminous GIC granites is proposed:

1) the upper part of a peraluminous, H_2O -undersaturated granodiorite magma stopped at a depth correspond to 300-400 MPa in the form of a crystalline mush. (This rheology is indicated by autolithic MME in G2M and by large anhedral quartz crystals, which are probably relics formed at greater depths);

2) the intrusive granodiorite body continued to differentiate with formation of melts (probably interstitial or within small pools) which were more acidic, peraluminous and had a composition similar to LGM;

3) subsequently, «collapse» of the external part of the almost solidified granodiorite magmatic mass, during transition from solid+melt to solid states, induced displacement of the more acidic and peraluminous melts towards the more external zones of the pluton (LGM dykes in G2M). L2M could represent a hybrid mixture of portions of the initial granodiorite (for example, plagioclase xenocrysts; Table 1) and of LGM-composition melt.

Peraluminous GIC granites were, in turn, intruded in the north western sector by a quartz diorite (QD) body which induced an apparently continuous thermometamorphic aureole of different grades within metapelitic wall rocks (fig. 1). Available data (Al-in hornblende geobarometry, cogenetic volcanic rocks nearby) indicate that this QD body was emplaced at about 100-200 MPa (Cozzupoli *et al.*, 1995; Cozzupoli *et al.*, 1997; Gaeta *et al.*, 1998). This indicates that GIC is a polybaric intrusive complex which formed during a 10-40 Ma time interval, according to presently available dates for QD adjacent to GIC (265 ± 5 Ma; Cozzupoli *et al.*, 1971a) and the range of radiometric ages for Sardinia granites (310-280 Ma, Poli *et al.*, 1989).

When radiometric dates and isotopic data will be available for all GIC lithotypes, it will

be possible to obtain a precise estimate of exhumation velocity and a more complete petrological model of this important sector of the Hercynian chain.

ACKNOWLEDGMENTS

The Authors acknowledge the critical review of the manuscript by Bernard Bonin, Carlos Villaseca, Francesca Tecce and Maria Luce Frezzotti. This work was conducted within the programs and with the financial support of CNR-Centro di Studio per gli Equilibri Sperimentali in Minerali e Rocce (CSESMR, Roma).

REFERENCES

- ABDEL-RAHMAN A.M. (1994) — *Nature of biotites from alkaline, calcalkaline and peraluminous magmas*. *J. Petrol.*, **35**, 525-541.
- ALTHAUS E., KAROTKE E., NITSCH K.H. and WINKLER H.G.F. (1970) — *An experimental re-examination of the upper stability limit of muscovite plus quartz*. *N. Jb. Mineral. Mh.*, **7**, 325-336.
- ANDERSON J.L. (1996) — *Status of thermobarometry in granitic batholiths*. *Trans. R. Soc. Edinburgh Earth Sci.*, **87**, 125-138.
- ASHWORTH J.R. and McLELLAN E.L. (1985) — *Textures*. In: *Migmatites* (Ashworth J. R. ed.). Glasgow: Blackie, 180-203.
- BODNARD R.J. and VITYK M.O. (1994) — *Interpretation of microthermometric data for H₂O-Cl fluid inclusions*. In: *Short Course of the Working group (IMA) Fluid inclusions in minerals: Methods and Applications* (De Vivo B. and Frezzotti M. L. eds). Virginia Tech, Blacksburg, 117-130.
- BROWN P.E. (1989) — *A microcomputer program for the reduction and investigation of the fluid inclusion data*. *Am. Mineral.*, **74**, 1390-1393.
- CARMICHAEL D.M. (1978) — *Metamorphic bathozones and bathograds: a measure of depth of post-metamorphic uplift and erosion on regional scale*. *Am. J. Sci.*, **278**, 769-797.
- CARMIGNANI L. (1996) — *Carta geologica della Sardegna 1:200.000*. Servizio Geologico Nazionale - Regione Autonoma della Sardegna. LAC, Firenze
- CARMIGNANI L., BARCA S., CAPPELLI B., DI PISA A., GATTIGLIO M., OGGIANO G. and PERTUSATI P.C. (1992) — *A tentative of geodynamic model for the Hercynian basement of Sardinia*. IGCP n. 276, Newsletter, **5**, 61-82.
- CAROSI R. and MALFATTI G. (1995) — *Analisi strutturale dell'unità di Meana Sardo e caratteri della formazione duttile nel Sarcidano-Barbagia di Seulo (Sardegna centrale, Italia)*. *Atti Soc. Tosc. Sci. Nat., Mem., Serie A*, **102**, 121-136.
- CHATTERJEE N.M. and JOHANNES W. (1974) — *Thermal stability and standard thermodynamic properties of synthetic 2M₁-muscovite, KAl₂[AlSi₃O₁₀(OH)₂]*. *Contrib. Mineral. Petrol.*, **20**, 244-267.
- COZZUPOLI D., DE FAZIO P., GAETA M. and NEGRETTI G. (1994) — *Lineamenti geopetrografici dei granitoidi peralluminosi del versante meridionale del Gennargentu, Sardegna (nota I)*. *Min. Petr. Acta*, **37**, 335-351.
- COZZUPOLI D., DE FAZIO P., GAETA M., MASSARO E. and NEGRETTI G. (1995) — *Le formazioni granitoidi del versante meridionale del Gennargentu, Sardegna (nota II): lineamenti geopetrografici dei granitoidi monzonitici*. *Min. Petr. Acta*, **38**, 25-39.
- COZZUPOLI D., GAETA M., MASTROBATTISTA P. and NEGRETTI G. (1997) — *Le formazioni granitoidi del Complesso Intrusivo del Gennargentu (Sardegna). Nota III: le metamorfite di contatto*. *Min. Petr. Acta*, **40**, 27-44.
- COZZUPOLI D., DISCENDENTI A., LOMBARDI G. and NICOLETTI M. (1971a) — *Cronologia K-Ar delle manifestazioni eruttive del settore di Seui-Seulo (Barbagia-Sardegna)*. *Per. Mineral.*, **40**, 113-124.
- COZZUPOLI D., DISCENDENTI A., LOMBARDI G. and NICOLETTI M. (1971b) — *Datazioni K-Ar di rocce granitoidi della Barbagia e dell'Ogliastra (Sardegna centro-orientale)*. *Per. Mineral.*, **41**, 311-325.
- DEBON F. and LE FORT P. (1983) — *A chemical-mineralogical classification of common plutonic rocks and association*. *Trans. R. Soc. Edinburgh Earth Sci.*, **73**, 135-149.
- DI VINCENZO G., ANDRIESEN P.A.M. and GHEZZO C. (1996) — *Evidences of two different components in a Hercynian peraluminous cordierite-bearing granite: the San Basilio intrusion (Central Sardinia, Italy)*. *J. Petrol.*, **37**, 1175-1206.
- DU BRAY (1994) — *Composition of micas in peraluminous granitoids of the eastern Arabian Shield*. *Contrib. Mineral. Petrol.*, **116**, 381-397.
- GAETA M., COZZUPOLI D., GAFÀ R.M., MISITI V. and NEGRETTI G. (1998) — *Anatectic structures in the thermal aureole of Gennargentu Igneous Complex (Sardinia, Italy)*. IAVCEI Int. Volcanol. Cong., Cape Town, South Africa, 11-16 July, 1998.
- GIORGETTI G., FREZZOTTI M.L. and GHEZZO C. (1992) — *Structural and microthermometric studies of fluid inclusions in the Gallura intrusive complex (N Sardinia)*. *Eur. J. Mineral.*, **4**, 1175-1185.

- GUILLOT S., LE FORT P., PECHER A., BARMAN M.R. and APRAHAMIAN J. (1995) — *Contact metamorphism and depth of emplacement of the Manaslu granite (central Nepal). Implications for Himalayan orogenesis*. *Tectonophysics*, **241**, 99-119.
- HOLTZ F. and BARBEY P. (1991) — *Genesis of peraluminous granites II. Mineralogy and chemistry of the Tourem Complex, North Portugal. Sequential melting vs restite unmixing*. *J. Petrology*, **32**, 959-978.
- HOLTZ F., JOHANNES W. and PICHAVANT M. (1992) — *Peraluminous granites: the effect of allumina on melt composition and coexisting minerals*. *Trans. R. Soc. Edinburgh Earth Sci.*, **83**, 409-416.
- JOHANNES W. and HOLTZ F. (1996) — *Petrogenesis and experimental petrology of granitic rocks*. Springer-Verlag, Berlin, 335 pp.
- KERRICK D.M. (1990) — *The Al_2SiO_5 polymorphs*. *Reviews in Mineralogy*, **22**, Mineralogical Society of America, 406 pp.
- KRETTZ R. (1983) — *Symbols for rock-forming minerals*. *Am. Mineral.*, **68**, 277-279.
- LE BAS M., LE MAITRE R., STRECKEISEN A. and ZANETTIN B. (1986) — *A chemical classification of volcanic rocks based on the total alkali-silica diagram*. *J. Petrology*, **27**, 745-750.
- MILLER C.F., STODDARD E.F., BRADFISH L.J. and WAYNE A.D. (1981) — *Composition of plutonic muscovite: genetic implications*. *Can. Mineral.*, **19**, 25-34.
- MUECKE G.K. and CLARKE D.B. (1981) — *Geochemical evolution of the South Mountain Batholith, Nova Scotia: rare-earth-element evidence*. *Can. Mineral.*, **19**, 133-145.
- PATTISON D.R.M. and TRACY R.J. (1991) — *Phase equilibria and thermobarometry of metapelites*. In: *Reviews in Mineralogy* **26**, Contact Metamorphism (Ferrick, D.M. ed.), Mineralogical Society of America, 105-206.
- PEARCE J.A., HARRIS N. B. and TINDLE A.G. (1984) — *Trace element discrimination diagrams for tectonic interpretation of granitic rocks*. *J. Petrology*, **25**, 956-983.
- PICHAVANT M., KONTAK D.J., HERRERA J.V. and CLARK A.H. (1988) — *The Miocene-Pliocene Macusani volcanics, SE Peru. I. Mineralogy and magmatic evolution of two-mica aluminosilicate-bearing ignimbrite suite*. *Contrib. Mineral. Petrol.*, **100**, 300-324.
- POLI G., GHEZZO C. and CONTICELLI S. (1989) — *Geochemistry of granitic rocks from the Hercynian Sardinia-Corsica batholith: Implication for magma genesis*. *Lithos*, **23**, 247-266.
- PUPIN J.P. (1980) — *Zircon and granite petrology*. *Contrib. Mineral. Petrol.*, **73**, 207-220.
- PUPIN J.P. (1988) — *Granites as indicators in paleogeodynamics*. *Rend. Soc. It. Mineral. Petrol.*, **43**, 237-261.
- RAIMBAULT L. and BURNOL L. (1998) — *The Richemont rhyolite dyke, Massif Central, France: a subvolcanic equivalent of rare-metal granites*. *Can. Mineral.*, **36**, 265-282.
- RICHARDSON S.W., GILBERT M.C. and BELL P.M. (1969) — *Experimental determination of kyanite-andalusite and andalusite-sillimanite equilibria: the aluminium silicate triple point*. *Am. J. Sci.*, **267**, 259-272.
- SCAILLET B., PICHAVANT M. and ROUX J. (1995) — *Experimental crystallization of leucogranite magmas*. *J. Petrology*, **36**, 663-705.
- SMITH J.V. and BROWN W.L. (1988) — *Feldspar minerals. 1 Crystals Structures, Physical, Chemical and Microtextural Properties*. Springer-Verlag, Berlin, Heidelberg, New York, pp. 828.
- STRECKEISEN A. (1976) — *To each plutonic rock its proper name*. *Earth Sci. Rev.*, **12**, 1-33.
- STUSSI J.M. and CUNEY M. (1993) — *Modèles d'évolution géochimique de granitoides peralumineux. L'exemple du complexe plutonique varisque du Millevaches Massif central français*. *Bull. Soc. Géol. Fr.*, **164**, 585-596.
- TOMMASINI S., POLI G. and HALLIDAY A.H. (1995) — *The role of sediment subduction and crustal growth in Hercynian plutonism: isotopic and trace element evidence from the Sardinia-Corsica Batholith*. *J. Petrology*, **36**, 1305-1332.
- TUTTLE O. and BOWEN N.L. (1958) — *Origin of granite in the light of experimental studies in the system $NaAlSi_3O_8$ - $KAlSi_3O_8$ - SiO_2 - H_2O* . *Geol. Soc. Am. Mem.*, **74**, 153 pp.
- VILLASECA C., BARBERO L. and ROGERS G. (1998a) — *Crustal origin of Hercynian peraluminous granitic batholiths of Central Spain: petrological, geochemical and isotopic (Sr, Nd) constraints*. *Lithos*, **43**, 55-79.
- VILLASECA C., BARBERO L. and HERREROS V. (1998b) — *A re-examination of the typology of peraluminous granite type in intracontinental orogenic belts*. *Trans. R. Soc. Edinburgh Earth Sci.*, **89**, 113-119.
- WILLIAMSON B.J., DOWNES H., THIRWALL M.F. and BEARD A. (1997) — *Geochemical constraints on restite composition and unmixing in the Velay anatectic granite, French Massif Central*. *Lithos*, **40**, 295-319.
- WYLLIE P.J. (1984) — *Constraints imposed by experimental petrology on possible and impossible magma sources and products*. *Phil. Trans. R. Soc. London*, **A310**, 439-456.